Vacuum 139 (2017) 37–43

Contents lists available at ScienceDirect

Vacuum

journal homepage: www.elsevier.com/locate/vacuum

Imaging and motion of cathode group spots during pulse-enhanced vacuum arc evaporation

Yinghe Ma [a], Chunzhi Gong [a, *], Xiubo Tian [a], Paul K. Chu [b]

[a] State Key Lab. of Advanced Welding and Joining, Harbin Institute of Technology, 150001 Harbin, China
[b] Department of Physics & Materials Science, City University of Hong Kong, Tat Chee Avenue, Kowloon, Hong Kong

ARTICLE INFO

Article history:
Received 25 October 2016
Received in revised form
3 December 2016
Accepted 8 February 2017
Available online 10 February 2017

Keywords:
Pulse enhanced vacuum arc
Cathode group spots
Pulse current
Nitrogen pressure

ABSTRACT

Pulse-enhanced vacuum arc evaporation (PEVAE) which combines pulsed and direct current operation of the arc source is a new approach in cathodic arc evaporation technology. One potential advantage is to deflect the arc along new paths over the target and prevent it from moving in only preferred areas. In this work, the cathode group spots (GSs) are photographed using a high-speed digital camera with exposure time of 100 μs and 25 ms and the influence of the pulse current and nitrogen pressure on the motion of the GSs including velocity and distribution are investigated. The experimental results reveal two types of GSs. With respect to the traditional DC arc current of 100 A, the GSs consist of a few fragments close to each other and for the PEVAE, and the GSs tend to organize in a roughly circular expanding ring. Quasi-quantitative analysis of the experimental results shows that a self-generated transverse magnetic field by the high pulsed arc current may bend and extend the GSs motion trajectory. It may also be related to the enhancement effect of the high pulse current on electron emission which can also contribute to the higher expansion speed of the GSs.

1. Introduction

The cathode arc is an excellent source of highly ionized metallic plasmas emitted at a high speed and is used in deposition of a variety of metallic layers including metal nitride, metal carbide, and metal oxide on tools and industrial parts. While direct-current power supplies are the simplest and cheapest power supplies, arc vaporization is also implemented depending on the melting point of the vaporized materials. Cathodic arcs tend to produce droplets or macroparticles which degrade the film properties and even lead to film delamination in serious cases. It is possible to reduce the amount of droplets in the vaporized materials by a magnetic field, filter [1], or refractory anode [2] or by optimizing instrumental parameters such as the gas flow rate or substrate bias [3]. Materials with a higher melting point may produce less and smaller droplets. Actually the style and parameters of arc also has important influence. The number of large droplets will be strongly diminished in HCA (high-current pulsed arc) deposition [4]. Afterwards M. Ellrodt et al. [5] have developed a new “modified pulse arc evaporation process” which represents a combination of both d.c. and pulse cathodic arcs. There are possibilities to improve the target consumption; to reduce the upper stability limit; even significant reductions in the quantity and size of the droplets have been observed from TiN and TiAlN layers [6]. Further using the name P3e™ [7], OC Oerlikon Balzers AG has prepared different oxide layer combinations using the pulsed cathodic arc and/or “dual pulsed arc” in an oxygen environment to enhance electron emission [8]. This method combines a large process window and low deposition temperature boding well for commercial application. In our previous work [9], a cathodic arc evaporation power supply was developed and the pulse enhanced electron emission arc process was investigated. The power supply is composed of a pulse emission unit and base current unit controlled by a computer with a touch screen. The experimental results demonstrate suppression of target poisoning, optimization of film structure, and reduction of macroparticles.

The spot motion is usually affected by the cathode geometry, arc current, reactive gas pressure, external magnetic field configuration, and other factors. Many cathode geometries exploiting the influence of the magnetic field on the spot motion have been suggested [10,11]. In the PEVAE process, the high pulse current which can induce a transverse self-magnetic field on the cathode surface is superimposed with an external magnetic field. This

* Corresponding author.
E-mail address: chunzhigong@163.com (C. Gong).

http://dx.doi.org/10.1016/j.vacuum.2017.02.008
0042-207X/

interaction may change the spot motion and the spot motion has been investigated in DC or pulsed arc mode. However, the cathode spots of PEVAE process has not been investigated experimentally in detail. The objective of this work is to further determine the motion velocity of the cathode spot and subsequent distribution in details at different pulsed current and nitrogen pressure, how the pulsed current is related to electron emission and the self-magnetic field, as well as the effects of the nitrogen pressure on the properties of the nitride layer on the cathode surface.

2. Experimental details and methodology

2.1. Experimental setup

The deposition system consisted of a cylindrical chamber reactor ($\Phi 1000 \times 1200$ mm^3) with pure Ti (100 mm of diameter) targets. The external applied transverse magnetic field is about 0.5 mT. The base pressure before deposition was fixed to 5.0×10^{-4} Pa by a turbo molecular pump and nitrogen was used as the reactive gas. The flow rate was adjusted by a mass flow controller and the working pressure in the chamber varied in the range between 1.0 and 2.5 Pa. An experimental PEVAE power supply was shown in Ref. [9]. The cathode spot motion was investigated in the PEVAE and DC arc modes, respectively. In the pulse operation mode, the arc was operated using a continuous base current of 50 A superposed with a pulse current of 150–400 A with a pulse width of 1 ms. The pulse frequency was adjustable to keep a constant average arc current of 100 A. The influence of the pulse current and nitrogen pressure on the cathode spot behavior was been investigated. The DC arc current was kept constant and the pulse arc current was varied in PEVAE process. And in the DC arc mode, the arc current was kept at 100 A. So the average arc current was same for PEVAE and DC arc modes.

2.2. Image processing

The cathode spots are usually difficult to observe, but one could image the light emission from these spots. Here, the cathode spot motion (macroscopic) was monitored by a high-speed video camera (HSVC) placed close to the observation window. The model was PhantomV311-32G, which temporal resolution is 1 μs A replaceable transparent protective layer was employed to avoid coating the observation window. An assembly of emission centers showed the fractal properties in the spatial and temporal dimensions [12]. To obtain the spot trace (a group of spots in ignition but not single-spot event), the exposure time was set as 100 μs and 25 ms, respectively. A short exposure time disclosed the spot motion more clearly, whereas a long exposure time smeared the image of fast changing spots but showed the overall trajectory. The approximate velocity of the spot could be determined by the length of the spot pathway in the photo divided by the exposure time. The length of the spot pathway was determined from the known diameter of the cathode target, 100 mm, as shown in Fig. 1. The actual length of the spot pathway was found to be reproducible to within ~10% and by using one characteristic bright point in the reference picture, the spatial distribution of the cathode spots could be obtained.

3. Experimental results

3.1. Motion of group spots observed from HSVC

Luminous group spots (GSs) with apparent diameters of 0.5–2 mm are observed in HSVC recording. Similar group spots are also observed with other arc currents as previously reported in Refs. [13–15]. As demonstrated by previous work [16,17], the spots sometimes extinguish and occasionally new spots appear from locations not adjacent to other spots. As the GSs proceed, they move and the characteristics depend on the cathode surface conditions, arc current, magnetic field, and so on. There are two types of motion for the GSs. The first type consists of a few fragments close to each other as shown in Fig. 1(a) for the 100 A DC arc current. With regard to the large pulsed arc current superposed with a small DC arc current, a second type GSs motion which tends to organize in a roughly circular expanding ring is observed as shown in Fig. 1(b) [pulsed arc of 400 A and DC arc of 50 A]. The temporal arc spots development corresponding to the time evolution of arc current pulse is shown in Fig. 2. During the high pulsed arc period, the GSs appear as an expanding ring with more fragments, while in the low DC arc period, the first type motion is observed since the individual fragments usually extinguish or break away from the circle at pulse-off and occasionally new ones appear. The observed maximum diameter (D) of the ring is about 23 mm which may increase with the pulsed arc current. Even the number of fragments increases with the pulsed arc current.

The motion of the GSs is featured by some fragments dying off and new ones appearing and so increasing the exposure time can help to observe the movement of more fragments and longer GSs trace. Fig. 3 presents the multiple GSs trace on the cathode surface at an exposure time of 25 ms. Fig. 3(a) shows that multiple GSs traces appear as a main branch for the DC arc. However for the PEVAE as shown in Fig. 3(b), the image of the GSs consists of a large branch periodically split into a few small branches having the appearance of small random fluctuation lines. These structures in the images suggest that the GSs trace consists of individual small fragments such as Fig. 1 each carrying high-density currents. Particularly, Fig. 3(b) shows that for the PEVAE at 25 m exposure time, the number of small branches is 4 which is equal to the number of pulsed arc because PEVAE 400 A corresponds to the pulsed arc frequency of 193 Hz. At the same time, the main traces resemble a circle and its maximum diameter ($\Phi 90$ mm) for DC arc is slightly bigger than the diameter ($\Phi 87$ mm) for the PEVAE. In particular, prior to apparent GSs splitting and after apparent macro-fragments merging, the GSs brightness increases considerably.

3.2. Arc current effect

The average velocity "v" of multiple GSs increases markedly with the arc current as shown in Fig. 4. The dependence is approximately linear for the pulsed arc but a surprisingly low "v" is observed from the DC arc. Similar results have been reported in Ref. [18]. For example, $v = 10.34$ m/s is measured for a DC arc current of 100 A while $v = 5.7$ m/s is measured for a DC arc current of 65 A in similar experiments. A high motion speed of GSs is effective in suppressing the production of macroparticles and improving the film quality and surface properties [19].

The morphology of the cathode GSs at different arc currents are shown in Table 1 and the pulse arc current has a critical effect on the cathode GSs trace. In the case of a DC arc, a big and approximately circular bright GSs trace appears from the cathode surface and the typical images are depicted in Figs. 1(a) and 2(a). In the case of a PEVAE arc, when pulsed arc current is 100 A, the GSs trace is similar that of DC arc. But with increasing pulsed arc current, there is an increasing tendency for the GSs to improve the luminance exhibiting a multiple branch structure and the cathode GSs pattern changes from a dim zigzag GSs trace [20] to one with brighter and more branches. It is more obvious that the number of sub-branches on the target surface corresponds to the frequency of the pulsed arc current when pulsed arc current is 300 or 400 A.

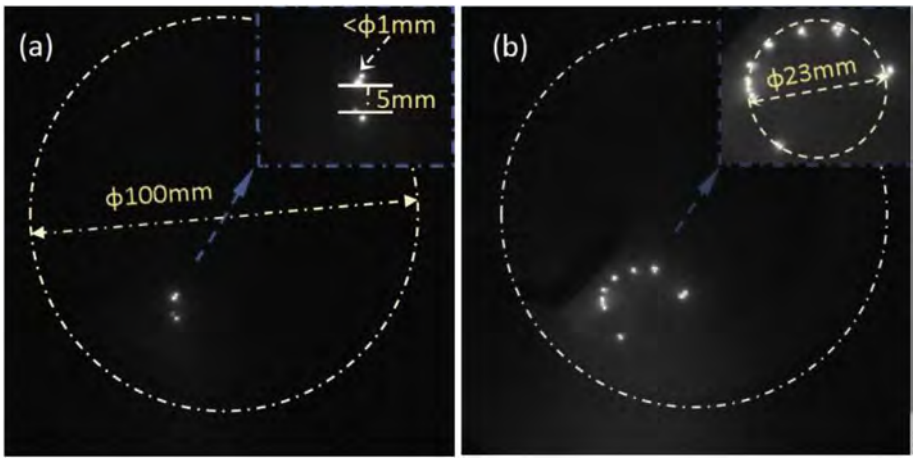

Fig. 1. Multiple GSs trace on the cathode surface (exposure time: 0.10 ms): (a) DC 100 A and (b) PEVAE 400 A.

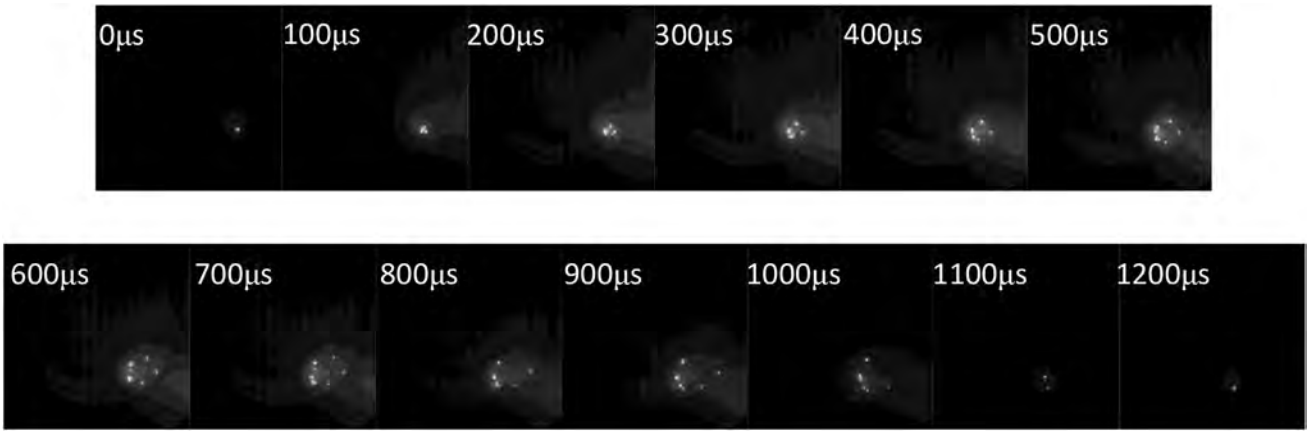

Fig. 2. Temporal arc spots development corresponding to the time evolution of arc current pulse.

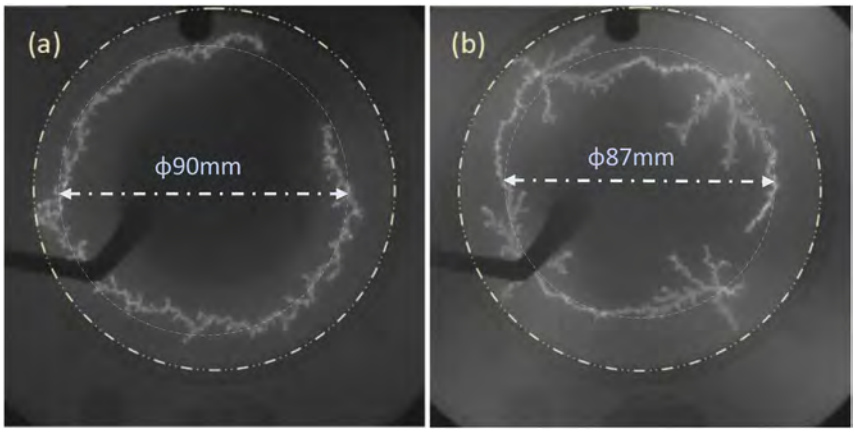

Fig. 3. Multiple GSs trace on the cathode surface (exposure time: 25 ms): (a) DC 100 A and (b) PEVAE 400 A.

3.3. N_2 pressure effect

The average velocity (v) of multiple GSs as a function of N_2 pressure is displayed in Fig. 5. This dependence is obtained by taking into account the frames in which multiple GSs appear. v increases slightly with N_2 pressure with increasing pulse arc currents and it may be related to surface poisoning by nitrogen. TiN with a higher melt point leads to locally unsteady arc burning and the arc spot moves away easily.

Table 2 shows the transient cathode GSs morphology at different N_2 pressure. Increasing the N_2 pressure has hardly any influence on the cathode GSs trace and improves the luminance of GSs slightly.

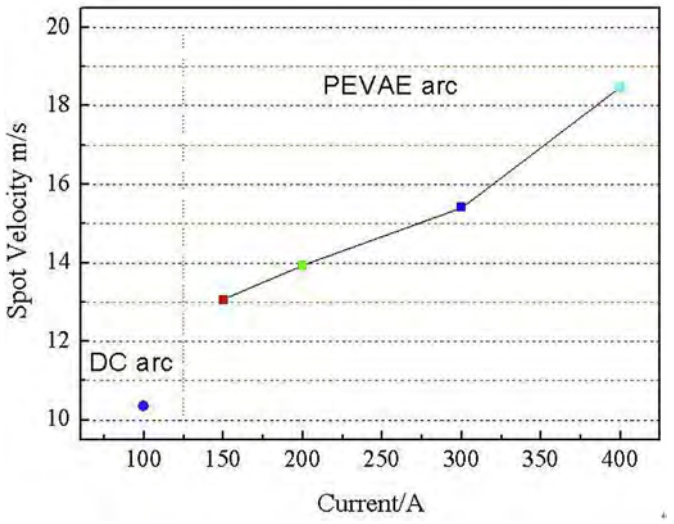

Fig. 4. Average velocity (v) of multiple GSs as a function of the arc current.

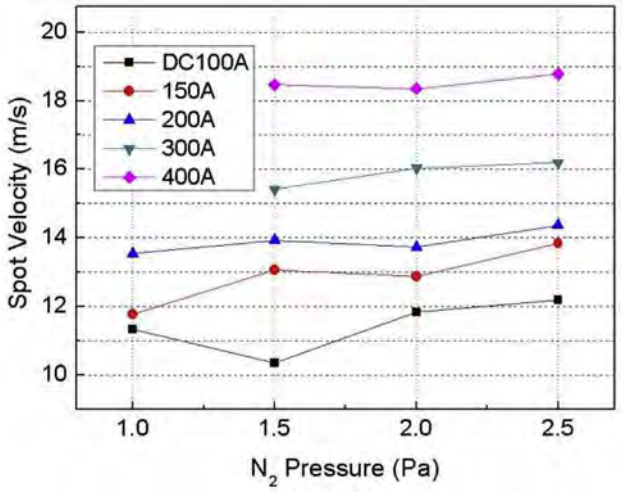

Fig. 5. Average velocity (v) of multiple GSs as a function on N_2 pressure with DC or different pulsed arc currents.

4. Discussion

A high pulsed current of the arc sources as well as utilization of low DC operation produce different GSs traces. The pulsed booster enhances electron emission and a small DC current helps to stabilize the cathodic arc discharge. Under these conditions, the cathode GSs can move more quickly and are distributed over the target area implying a uniform removal potential of the target materials in accordance with previous results [8]. The enhanced electron emission, one of most attractive features of PEVAE discharge, may affect the plasma density and distribution and change the behavior of arc spots. Meanwhile, the current in the cathode plasma jet of a vacuum arc produces a self-magnetic field which is superimposed with the external magnetic field. Likewise, the self-magnetic field is produced in the PEVAE since a higher pulse current is utilized. This self-magnetic field is variable due to the adjustable modulation of the pulse and DC currents consequently affecting the spot movement. Moreover, the difference in the physical nature of spot types is related to the degree of contamination of the cathode [21]. A micro explosion occurs primarily on the energetically favorable cathode sites, that is, where dielectric films are present [22].

4.1. Influence of enhanced electron emission

The number of splitting spots as a function of arc currents at different N_2 pressure is presented in Fig. 6. The number of splitting spots depends on the arc pulsed current and the GSs tend to split at higher currents in PEVAE discharging. The appearance of the GSs motion, such as the temporal and spatial distribution of ignition, appears to be better interpreted by a fractal than by the long-anticipated "true" value [23]. Here, the GSs behavior seemingly obeys the cell theory [24–26].

The cathode spot of a vacuum arc exists as a single cell at currents ranging from the threshold current i_{th} to $2i_{th}$ and tends to split at larger currents [27,28]. Thus, for the current carried by a stable cell, we have $i_c \approx 2i_{th}$. For $i \gg i_{th}$ the number of cells is $L = i/2i_{th}$. It can be understood that the number of splitting spots increases with pulsed current in the PEVAE process. Compared to the DC arc, the PEVAE discharge produces a large amount of emitting electrons to excite more emission sites as shown in Fig. 7. More GSs are ignited and operated electrically in parallel compete for the available current and associated power dissipation [29,30]. The larger the arc pulsed current, the more the emitting electrons and the more easily ignition occurs [31]. This shortens the individual GSs active stage leading to fast GSs motion as shown in Fig. 4 and the random sub-branches in Table 1.

All of apparent GSs except one become extinct when the pulsed current pauses while new apparent GSs split again when the next pulsed current comes as shown in Fig. 3(b). Consecutive GSs formation appears as displacement with momentary velocities up to about 18 m/s in PEVAE (400 A). The GSs dynamics leads to random displacement of the crater center and the arc behavior may be approximated by cumulating multiple GSs traces as shown in Table 3. The coverage ratio of GSs on target was about 55.6% in DC arc mode while it could increase to about 70.3% in PEVAE mode. The high coverage of GSs on target surface will lead to high target utilization rate.

Table 1
Visual observation of multiple GSs traces on the cathode surface at different arc currents.

DC arc	PEVAE: pulsed arc current (superposed with DC 50 A; 1.5Pa)			
100 A	150 A	200 A	300 A	400 A
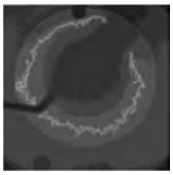	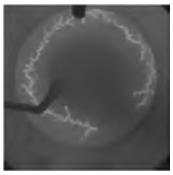	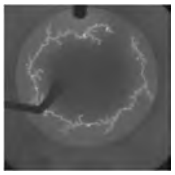	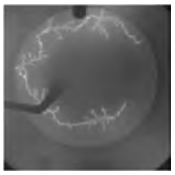	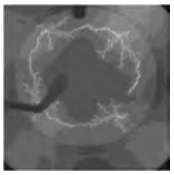

Table 2
Visual observation of multiple GSs traces on the cathode surfaces at different N_2 pressure.

	N_2 Pressure			
	1.0 Pa	1.5 Pa	2.0 Pa	2.5 Pa
DC arc (100 A)	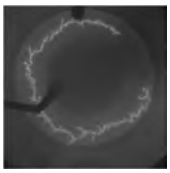	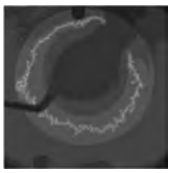	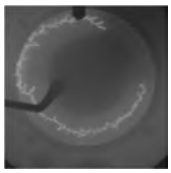	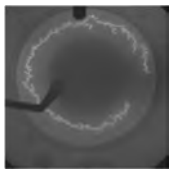
PEVAE (Pulsed 400 A DC 50 A)	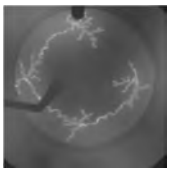	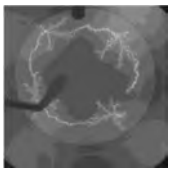	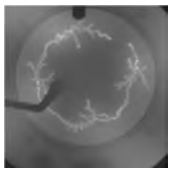	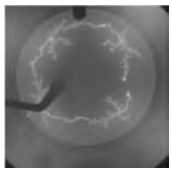

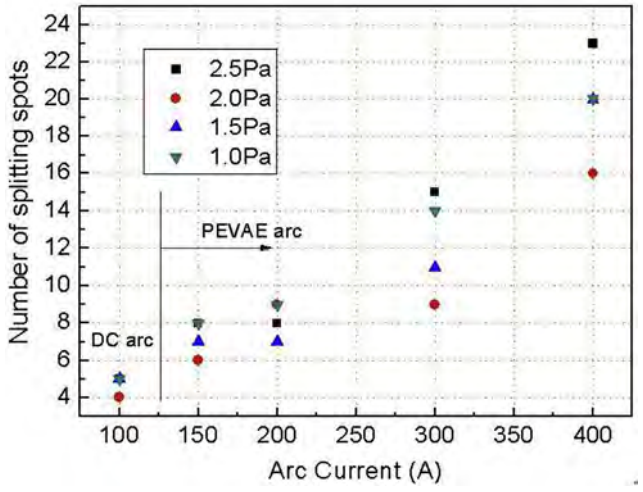

Fig. 6. Number of splitting spots as a function on arc currents at different N_2 pressure.

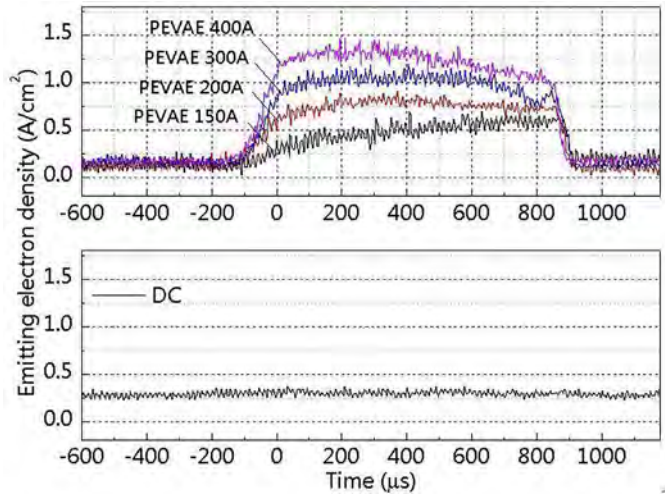

Fig. 7. Emitting electron density as a function on arc currents at N_2 pressure of 1.5 Pa.

4.2. Influence of self-magnetic field

D Y Fang [32] has developed a satisfactory model for the retrograde motion mechanism of vacuum arcs, in which the arc velocity should increase with increasing magnetic induction etc. Only for high arc current the theoretically calculated arc velocities are smaller than the experimentally measured data, the reason of this disagreement seems to be that the effect of the self-magnetic field of the arc current has not been taken into consideration.

In the high-current vacuum arc without an externally applied transverse magnetic field, B_t is the azimuthal magnetic field generated by the arc current and can be calculated by Eq. (1) as follows:

$$B = \int_0^L dB = \frac{\mu_0}{4\pi} \int_0^L \frac{Idl \times r}{r^3}. \tag{1}$$

In the DC current stage for PEVAE or traditional DC arc discharge, the spots are grouped closer together as shown in Fig. 1(a). Here it can be simplified to a dot fragment with a diameter of d such as $d = 2r \approx 5\ mm$ in Fig. 1(a). This expression differs from expression for a direct wire with a current by a factor 1/2 because the linear currents extend only in the half space above the cathode surface [33]. Thus the self-magnetic field can be calculated by Eq. (2):

$$B = \frac{\mu_0}{4\pi r} I \tag{2}$$

In the pulsed current stage in the PEVAE discharge, the GSs appear as an expanding ring and the self-magnetic field can be approximately calculated by Eq. (3) [Refs. [34–36]]:

$$B_t(t) \approx \frac{\mu_0 I(t)}{4\pi R(t)} \approx \frac{\mu_0}{2v} \cdot f \cdot I_p \tag{3}$$

where $I(t) \approx di/dt \cdot t \approx 2\pi \cdot f \cdot I_p \cdot t$ is the arc current in the initial expansion stage, $R(t) \approx v \cdot t$ is the radius of the GSs expansion ring, and v is the GSs expansion speed obtained experimentally for different peak pulsed currents. For example, in PEVAE, the self-magnetic field $B_t \approx 2\mu_0 \approx 2.5 \times 10^{-3}\ mT$ on the DC current stage and $B_t \approx 2000\mu_0 \approx 2.52\ mT$ on the pulsed current stage (400 A), so the total transverse magnetic field is about 0.5 mT or 3 mT respectively.

The magnetic pressure difference and pressure gradient may

Table 3
Cumulative multiple GSs traces on the cathode surfaces at different arc currents.

DC arc	PEVAE: pulsed arc current (superposed with DC 50 A; 1.5 Pa)			
100 A	150 A	200 A	300 A	400 A
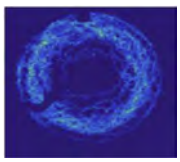	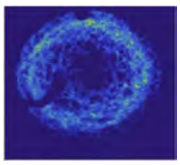	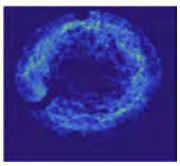	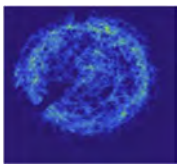	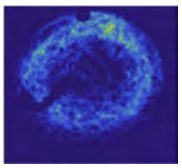

Table 4
Cumulative multiple GSs traces on the cathode surfaces at different N_2 pressure.

	N_2 Pressure			
	1.0 Pa	1.5 Pa	2.0 Pa	2.5 Pa
DC arc (100 A)	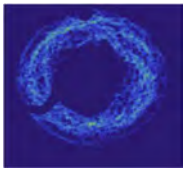	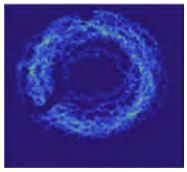	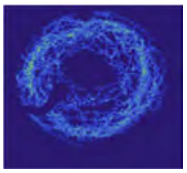	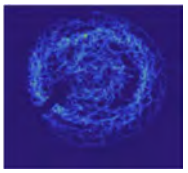
PEVAE (Pulsed 300 A DC 50 A)	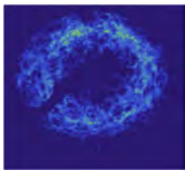	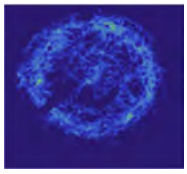	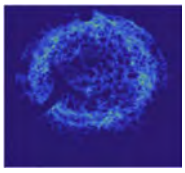	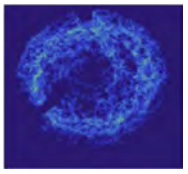

increase with the self-magnetic field and external field in the multiple cathode spot regimes [37]. The probability for new spot ignition on the retrograde side likewise increases, so that the directed retrograde spot velocity increases. Our results are in agreement with the observations in Ref. [38] in which the velocity increases nonlinearly with magnetic field showing asymptotic behavior at large values of B_t (>12 mT) to a value. On the other hand, for a relatively strong externally applied magnetic field, the variable self-magnetic field further inflects the magnetic field line [39] and the GSs break away from the confined circular trajectory [40]. It is also the reason for the sub-branch existence and higher probability of large surface erosion area in the PEVAE.

4.3. Influence of cathode surface nitride layer

There are two mechanisms, charging of the dielectric films and inclusion present on the cathode and due to the enhancement in the current density at the cathode micro protrusions. These mechanisms are responsible for the two types of vacuum arc spots. In the PEVAE discharge, the latter is predominant when pulse current is large due to enhanced electron emission. The former effect is not significant since the TiN layer is conductive (~20 mΩ m) [18]. The velocity increases slightly with increasing N_2 pressure as shown in Fig. 4. The enhanced mobility may be related to the layer on the cathode surface [41]. The TiN layer with a high melting point is difficult to remove and has a low conductivity compared to the Ti cathode. There results in the arc spot being preferentially on the nitride surface. Table 4 shows the cumulative multiple GSs traces on the cathode surface for different N_2 pressure. The results indicate that the arc moves more uniformly at a higher pressure and once again PEVAE gives rise to surface erosion of the entire surface.

5. Conclusion

Cathode spot motion in the PEVAE and DC arc discharge is monitored and discussed. The enhanced electron emission and self-magnetic field increase the GSs expansion speed and broaden the GSs distribution. The speed of GSs increases from 13.1 m/s to 18.4 m/s as the pulse current is raised from 150 A to 400 A. A higher N_2 pressure increases the GSs motion slightly giving rise to uniform surface erosion. The arc behavior of the GSs is different. For the DC arc, the GSs consist of a few fragments close to each other whereas for the PEVAE, the GSs tend to organize in a roughly circular expanding ring. The GSs motion shows that the arc moves along new paths over the target and prevents it from only moving in the preferred areas. The results indicate PEVAE is beneficial to high target utilization rate.

Acknowledgements

The authors gratefully acknowledge the financial support of this research from National Natural Science Foundation of China (No. U1330110, 11675047 and 51175118) and City University of Hong Kong Applied Research Grant No. 9667122.

References

[1] H. Takikawa, H. Tanoue, IEEE Trans. Plasma Sci. 35 (2007) 992.
[2] I.I. Beilis, Y. Koulik, R.L. Boxman, D. Arbilly, J. Mater. Sci. 45 (2010) 6325.
[3] M. Ali, E. Hamzah, T. Abbas, M.R.H.J.M. Toff, I.A. Qazi, Surf. Rev. Lett. 15 (2008) 653.
[4] P. Siemroth, T. Schukke, T. Witke, Surf. Coat. Technol. 68–69 (1994) 314.
[5] M. Ellrodt, H. Mecke, Surf. Coat. Technol. 74–75 (1995) 241.
[6] M. Buschel, W. Grimm, Surf. Coat. Technol. 142–144 (2001) 665.
[7] Rudigier, United States Patent, US 2011/0278157 A1.

[8] J. Ramm, M. Ante, T. Bachmann, B. Widrig, H. Brändle, M. Döbeli, Surf. Coat. Technol. 202 (2007) 876.
[9] Y.H. Ma, X.B. Tian, M.Z. Cai, W.L. Sun, Y. Kong, R. Kou, C.Z. Gong, Vac. (in China) 51 (2014) 31.
[10] K.K. Zabello, Y.A. Barinov, A.M. Chaly, A.A. Logatchev, S.M. Shkol'nik, IEEE Trans. Plasma Sci. (2005) 331553.
[11] A. Anders, Springer (2008) 114.
[12] M.S. Bieniek, P.G.C. Almeida, M. S Benilov, J. Phys. D Appl. Phys. 49 (2016) 105201.
[13] A.M. Chaly, A.A. Logatchev, S.M. Shkolnik, IEEE Trans. Plasma Sci. 25 (1997) 564.
[14] S. Kajita, D. Hwangbo, N. Ohno, M.M. Tsventoukh, S.A. Barengolts, J. Appl. Phys. 116 (2014) 233302.
[15] I.I. Beilis, B. Sagi, V. Zhitomirsky, R.L. Boxman, J. Appl. Phys. 117 (2015) 233303.
[16] I. Beilis, B. E Djakov, B. Juttner, H. Pursch, J. Phys. D Appl. Phys. 30 (1997) 119.
[17] B.E. Djakov, B. Juttner, J. Phys. D Appl. Phys. 35 (2002) 2570.
[18] I. Zhirkov, A. Petruhins, J. Rosen, Surf. Coat. Technol. 28 (2015) 120.
[19] P.D. Swift, J. Phys. D Appl. Phys. 29 (1996) 2025.
[20] B. Juttner, I. Kleberg, J. Phys. D Appl. Phys. 33 (2000) 2025.
[21] A.E. Guile, B. Jüttner, PS-8 260, IEEE Trans. Plasma Sci. (1980).
[22] G.A. Mesyats, M.B. Bochkarev, A.A. Petrov, S.A. Barengolts, Appl. Phys. Lett. 104 (2014) 184101.
[23] A. Anders, IEEE Trans. Plasma Sci. 33 (2005) 1456.
[24] B.E. Djakov, R. Holmes, J. Phys. D Appl. Phys. 4 (1971) 504.
[25] G.A. Mesyats, IEEE Trans. Plasma Sci. 23 (1995) 879.
[26] S.A. Barengolts, G.A. Mesyats, D.L. Shmelev, IEEE Trans. Plasma Sci. 31 (2003) 809.
[27] G.A. Mesyats, IEEE Trans. Plasma Sci. 41 (2013) 676.
[28] M.A. Gashkov, N.M. Zubarev, O.V. Zubareva, G.A. Mesyats, I.V. Uimanov, J. Exp. Theor. Phys. 122 (2016) 776.
[29] I.I. Beilis, IEEE Trans. Plasma Sci. 27 (1999) 821.
[30] J. Lun, R.T. Dobson, W.H. Steyn, J. Propuls. Power 26 (2010) 663.
[31] G.A. Mesyats, N.M. Zubarev, J. Appl. Phys. 113 (2013) 203301.
[32] D.Y. Fang, J. Phys. D Appl. Phys. 15 (1982) 833.
[33] B.E. Djakov, R. Holmes, IEE Int. Gas Discharge Conf. London, 1970, pp. 468–472.
[34] X.C. Song, Z.Q. Shi, C. Liu, S.L. Jia, L.J. Wang, IEEE Trans. Plasma Sci. 41 (2013) 2061.
[35] N.E. Perskii, V.I. Sysun, Y.D. Khromoi, TVT 27 (1989) 1060.
[36] Z.Q. Shi, X.C. Song, C. Wang, S.L. Jia, L.J. Wang, IEEE Trans. Plasma Sci. 42 (2014) 2124.
[37] I.I. Beilis, Appl. Phys. Lett. (2002) 813935.
[38] P.D. Swift, D.R. McKenzie, I.S. Falconer, P.J. Martin, J. Appl. Phys. 66 (2) (1989) 505–512.
[39] L.P. Harris, PS-11 94, IEEE Trans. Plasma Sci. (1983).
[40] H.O. Schrarde, IEEE Trans. Plasma Sci. 17 (1989) 635.
[41] M. Ellrodt, M. Kuhn, Contrib. Plasma Phys. 36 (1996) 687.